

1 **Authors**

2 Steffen Mischke^{1,2}, Ulla Schudack², Sébastien Bertrand^{3,4}, Suzanne A. G. Leroy⁴

3

4 ¹Institute for Earth and Environmental Sciences, University of Potsdam, 14476 Potsdam,
5 Germany

6 ²Institute of Geological Sciences, Freie Universität Berlin, 12249 Berlin, Germany

7 ³Alfred Wegener Institute for Polar and Marine Research, Marine Geology and Paleontology,
8 27520 Bremerhaven, Germany

9 ⁴Department of Geography and Earth Sciences and Institute for the Environment, Brunel
10 University, West London, Uxbridge UB8 3PH, UK

11

12 **Title**

13 Ostracods from a Marmara Sea lagoon (Turkey) as tsunami indicators

14

15

16 Corresponding author: Steffen Mischke (smischke@zedat.fu-berlin.de)

17

18

19 **Key words**

20 Marmara Sea; Gulf of İzmit; Ostracoda; lagoon; brackish water; tsunami

21

22 **Abstract**

23 A 352 cm long sediment core from Hersek Lagoon (Gulf of İzmit) was investigated for its
24 ostracod species composition in order to evaluate the potential of ostracods to detect
25 tsunami deposits in coastal environments. The Gulf of İzmit is the eastern bay of the
26 Marmara Sea which is tectonically controlled by the North Anatolian Fault. Ostracod shells
27 are rare in the lower third of the core, which probably represents a coastal wetland
28 environment. According to radiocarbon dating of terrestrial plant remains, this unit was
29 deposited between AD 500 and AD 800. Above, ostracod shells are abundant and
30 dominantly monospecific, composed almost exclusively of the widespread brackish water
31 ostracod *Cyprideis torosa*. This almost monospecific occurrence indicates the establishment
32 and maintenance of the Hersek Lagoon after AD 800. Three distinct layers of mollusc shells
33 and fragments contain ostracod shells of marine and to a lesser extent non-marine origin in
34 addition to those of *Cyprideis torosa*. The shell layers are further characterized by significant
35 maxima in total ostracod shell numbers. The high concentration of ostracod shells, the higher
36 species numbers and the mixture of marine, lagoonal and non-marine ostracod shells shows
37 that shell layers were formed as high-energy deposits resulting from tsunamis or large
38 storms in the Marmara Sea. The partial occurrence of non-marine ostracod shells in the shell
39 layers possibly indicates that tsunamis with extensive run-ups and significant backwash flows
40 caused the high-energy deposits rather than large storms. The investigated sediments show
41 that lagoonal ostracods can serve as good proxies for tsunamis or large storms through
42 significant variations in total shell numbers, species numbers and the mixing of shells of
43 different origin.

44

45 **1. Introduction**

46 Tsunamis and large storms are significant threats to coastal population and infrastructure.
47 Precautionary/mitigation measures were intensively discussed following the devastating
48 tsunami in the Indian Ocean on 26 December 2004, and hurricane Katrina that destroyed

49 large parts of New Orleans in August 2005. The risk assessment of specific coastal regions
50 often relies on systematic records of tides and meteorological data although the
51 observational data do not necessarily cover periods of tsunami occurrence. Less systematic
52 records such as historical documents and, eventually, geological evidence is required to
53 obtain longer records for long-term assessment of catastrophic risks by tsunamis and storms
54 (i.e. Leroy et al., 2010).

55 Consequently, several examples of tsunami or storm reconstructions based on geological
56 evidence were presented in recent years (e.g., Leroy et al., 2002; Maramai et al., 2005;
57 Dominey-Howes, 2007; Fujino et al., 2009). Sedimentological features such as erosional
58 contacts, normally graded beds, rip-up clasts or boulders and organism remains were used
59 for the reconstruction of catastrophic flooding as a result of tsunamis or large storms in
60 coastal regions (Dawson and Smith, 2000; Dawson and Stewart, 2007; Morton et al., 2007;
61 Dahanayake and Kulasena, 2008, Donato et al., 2008). Foraminifera and diatom tests are
62 thought to be the most significant biotic indicators for the identification of tsunami and storm
63 deposits (Clague et al., 1999; Dawson and Smith, 2000; Dawson, 2007; Kortekaas and
64 Dawson, 2007; Dahanayake and Kulasena, 2008). In contrast, ostracods, which represent
65 one of the most widespread organism groups that produces readily fossilized remains, have
66 only rarely been used for the recognition of tsunami and storm deposits (Fujiwara et al.,
67 2000; Ruiz et al., 2005, 2010; Boomer et al., 2007; Alvarez-Zarikian et al., 2008). Ostracods
68 may however provide more information than foraminifers in coastal water bodies with low
69 salinity or freshwater inflow. In comparison to diatoms, ostracods may be more efficiently
70 **used** since sample processing is usually less laborious. In addition, the possibility to perform
71 stable isotope and trace element analyses on the calcitic ostracod shells may represent a
72 significant advantage over diatoms and some groups of foraminifers (Frenzel and Boomer,
73 2005). Therefore, we examined the potential of ostracods as indicators of tsunamis and large
74 storms using a sediment core from Hersek Lagoon at the southeastern Marmara Sea shore

75 (Gulf of İzmit, Turkey). Additional results and those of other cores from the lagoon are
76 presented in a separate paper by Bertrand et al. (submitted).

77

78 **2. Study area**

79 Hersek Lagoon is located on a northward-prograding delta (Hersek Delta or Hersek
80 Peninsula) in the Gulf of İzmit of the eastern Marmara Sea (Turkey, Fig. 1). The area of the
81 lagoon is 1.4 km² and the water depth ranges between 0.3 and 0.7 m. The salinity is 28-30
82 P.S.U. in most parts of the lagoon, and 38-40 P.S.U. at its northwestern margin. The lagoon
83 is separated from the sea by a narrow sand ridge reinforced by a concrete dike in the last
84 century. The topography in the vicinity of the lagoon is flat (2-3 m above sea level [asl])
85 except for a prominent hill of uplifted Pleistocene marine sediments at the northern tip of the
86 peninsula (Fig. 1). The climate is characterized by dry summers and mild and rainy winters.
87 The Gulf of İzmit is the eastern extension of the Marmara Sea, which connects the
88 Mediterranean Sea in the south to the Black Sea in the north. The water in the Marmara Sea
89 is permanently stratified, with a halocline at 20-25 m depth. Less saline (salinity: 18) surface
90 water of the Black Sea flows to the Aegean Sea and saline bottom water (38) flows in the
91 opposite direction (Ünlüatu et al., 1990). Water depth in the western and central Gulf of İzmit
92 basins near the Hersek Peninsula reaches ca 200 m but does not exceed 50 m in the close
93 vicinity of the delta (Dolu et al., 2007; Fig. 1).

94 The tectonic setting in the Marmara Sea region is mainly controlled by the North Anatolian
95 Fault Zone (NAFZ), which is one of the longest and most active strike-slip faults in the world
96 (Fig. 1). The NAFZ runs roughly parallel to the Black Sea coast of Anatolia and splits into two
97 strands in its western part (Fig. 1). The northern strand passes through the Gulf of İzmit and
98 Hersek Lagoon (Yalova fault segment) and runs further through the Marmara Sea,
99 representing the source of numerous large historical earthquakes (Dolu et al., 2007; Fig. 1).

100 The most recent major earthquake of the NAFZ (17 August 1999) triggered surface ruptures

101 including vertical displacements, submarine slumps and eventually a devastating tsunami in
102 the Gulf of İzmit (Tinti et al., 2006).

103

104 **3. Materials and methods**

105 Ten cores were obtained with a Livingstone piston corer from an anchored raft in Hersek
106 Lagoon. Core HK04LV5 (40.724°N, 29.519°E, 0.47 m water depth), which is one of the
107 longest cores collected and the only one from a position north of the Yalova segment of the
108 North Anatolian Fault, was selected for ostracod analysis.

109 Samples of about 65 g were collected continuously from 5 cm segments of a core half for
110 ostracod analysis and sieved with 500, 250 and 63 μm meshes. Absolute ostracod shell
111 abundances and the presence of mollusc shells and fragments, and charred and non-
112 charred plant remains were determined with a low-power binocular microscope. Up to 300
113 ostracod shells were counted and picked from the sieve residues of the $>250 \mu\text{m}$ fraction.
114 For samples containing more than 300 shells, randomly selected subsamples of the
115 remaining sieve residue material were used for further counting and total shell abundances
116 were then calculated by extrapolation. Identification of ostracod species mainly followed
117 Athersuch et al. (1989). Shells of the less frequent species were only identified with
118 reservation due to their low numbers and occurrence at juvenile stages.

119 Grain size was estimated by measuring the volume of sediment in the fractions obtained
120 after sieving at 500, 250 and 63 μm .

121 Radiocarbon dating was performed on terrestrial plant remains from four stratigraphic levels
122 (334-329 cm, 215-210 cm, 102.5-97.5 cm, 45-40 cm; Fig. 2). Samples were analyzed at the
123 Poznan Radiocarbon Laboratory, Poland, and the radiocarbon ages were calibrated with
124 OxCal 4.0 using the IntCal04 calibration curve (Reimer et al., 2004).

125

126 **4. Results**

127 Radiocarbon dating yielded the following ages: 1590 ± 80 ^{14}C a BP at 334-329 cm, 1230 ± 60
128 ^{14}C a BP at 215-210 cm, 1190 ± 30 ^{14}C a BP at 102.5-97.5 cm and 1235 ± 35 ^{14}C a BP at 45-
129 40 cm. The corresponding weighted averages of calibrated ages are AD 511, 792, 834 and
130 777, respectively.

131 Recovered sediments mainly comprise homogenous mud (Fig. 2). Laminations, organic-rich
132 sediments, and four distinct sand layers occur in the lower third of the core. Three layers of
133 brackish-marine mollusc shells and fragments were recorded in the upper half of the core.

134 The grain size fraction $<63 \mu\text{m}$ predominates with a mean proportion of 77 %. The fractions
135 $63\text{-}250 \mu\text{m}$, $250\text{-}500 \mu\text{m}$, and $>500 \mu\text{m}$ have mean proportions of 10 %, 4 % and 9 %. The
136 finest ($<63 \mu\text{m}$) and coarsest ($>500 \mu\text{m}$) fractions have a relatively large variability compared
137 to the intermediate fractions (Fig. 2). Grain size changes are only shown for the $> 500 \mu\text{m}$
138 fraction since the $63\text{-}250 \mu\text{m}$ and $250\text{-}500 \mu\text{m}$ fractions are relatively stable, and the $<63 \mu\text{m}$
139 fraction shows an opposite but otherwise similar trend (Fig. 2).

140 Ostracod shells are almost absent from the lower part of the core but abundant in its upper
141 half (Fig. 2). Shells of *Cyprideis torosa* clearly predominate whereas those of *Loxoconcha*
142 *elliptica*, *L. cf. rhomboidea* and *Heterocypris salina* are restricted to a number of stratigraphic
143 levels (Fig. 2, Plate 1). All shells of *Cyprideis torosa* belong to the smooth form *Cyprideis*
144 *torosa* forma *littoralis* apart from a single noded shell (*Cyprideis torosa* forma *torosa*)
145 recorded at 40-35 cm depth (Fig. 2, Plate 1). Those of *Pontocythere* sp., *Aurila* cf.
146 *arborescens*, *Eucyprinotus* cf. *rostratus* display a more erratic occurrence. Total numbers of
147 ostracod taxa and total shell concentrations peak at three levels in the core: 153-142 cm, 98-
148 87 cm and 38-27 cm (Fig. 2).

149 Mollusc shells and fragments occur in all samples above 213 cm, charred plant remains
150 occur between 294 and 242 cm, and non-charred plant remains were observed between 243
151 and 172 cm (Fig. 2). Charophyte gyrogonites were recorded at 97 and 47 cm core depth, and
152 in two adjoining samples at 32 and 27 cm (Fig. 2).

153

154 **5. Discussion and conclusion**

155 Calibrated ages of the four samples analyzed for radiocarbon indicate that the sediment was
156 deposited between ca AD 500 and 800. The upper three samples yielded virtually identical
157 ages, most likely reflecting particularly high accumulation rates in at least the upper 215 cm
158 of the core. Alternatively, the incorporation, transportation and accumulation of aged
159 terrestrial organic matter of similar source over a longer period of time could have caused the
160 similar age results for the upper three ¹⁴C samples.

161 The most striking feature of the core from Hersek Lagoon is the predominance of ostracod
162 shells of *Cyprideis torosa* in its upper 185 cm. *Cyprideis torosa* is a widespread inhabitant of
163 brackish coastal waters of the northern hemisphere with a salinity tolerance ranging from
164 almost pure freshwater to hyperhaline conditions (Meisch, 2000). *Cyprideis torosa* is the
165 most abundant species in the Baltic Sea (Frenzel and Boomer, 2005) and it often inhabits
166 lagoons and estuaries of the Mediterranean Sea alone and at high concentrations (Meisch,
167 2000; Ruiz et al., 2000). It was the only species recorded in all of the eight lagoons of Turkey
168 examined by Altinsaçlı (2004) including two lagoons of the Marmara Sea coast. Furthermore,
169 it frequently occurs in brackish continental waters in northern Africa, the Near East and
170 Central Asia (Meisch, 2000; Mischke et al., 2010). Although commonly occurring in the
171 present Marmara Sea and the Gulf of İzmit, *Cyprideis torosa* seldom predominates (Kubanç
172 et al., 1999; Kubanç, 2005). Its dominance in the recovered sediments is evidence that
173 Hersek lagoon was separated from the Marmara Sea during the period represented by the
174 middle and upper part of the core.

175 In contrast, the lowermost part of the core (352-223 cm) is characterized by only sporadic
176 occurrences of ostracod and mollusc shells in low numbers, and more silty and organic-rich
177 sediments with charred plant remains probably representing a coastal wetland environment.
178 Sediment samples between 223 and 172 cm all contain shells of *Cyprideis torosa* although in
179 low numbers, mollusc shells and fragments, and non-charred instead of charred plant
180 remains, probably representing the establishment of a lagoon with a high sediment influx

181 during its initial stage. This interpretation is supported by geochemical data from the core
182 (Bertrand et al., submitted).

183 Three distinct layers of brackish-marine mollusc shells and fragments occur at ca 150, 90
184 and 30 cm core depth, within the homogenous mud that composes the upper part of the core
185 (Fig. 2). All three shell layers contain shells of *Loxoconcha elliptica* and *Loxoconcha* cf.
186 *rhomboidea* beyond those of *Cyprideis torosa*. In addition, a few more erratically occurring
187 ostracod species are apparently confined to these shell layers (Fig. 2, Plate 1). The ostracod
188 shell concentration reaches three pronounced maxima corresponding to increases in the
189 number of ostracod taxa in the shell layers. *Loxoconcha elliptica* is a typical brackish water
190 species inhabiting estuaries, lagoons and pools, commonly associated with algae and mud
191 (Athersuch et al., 1989). *Loxoconcha rhomboidea* is a predominant species in the near-shore
192 waters of the southern Marmara Sea and other species of *Loxoconcha*, *Aurila* and
193 *Xestoleberis* occur in this region too (Kubanc, 2005). Furthermore, *Loxoconcha rhomboidea*
194 and other species of *Loxoconcha*, *Xestoleberis* sp., *Pontocythere* sp. and *P. elongata*, and
195 *Aurila* sp. were recovered from Pleistocene marine sediments in the Gulf of İzmit in the north
196 of Hersek Peninsula. Thus, shells of *Loxoconcha rhomboidea*, *Xestoleberis*, *Pontocythere*
197 and *Aurila* in the Hersek Lagoon sediments probably originate from the Gulf of İzmit section
198 of the Marmara Sea.

199 In contrast, *Heterocypris salina* and *Eucyprinotus* cf. *rostratus* are typical non-marine
200 ostracod species (Fig. 2, Plate 1). *Heterocypris salina* is an abundant inhabitant of small
201 slightly brackish coastal water bodies of the Baltic and North Sea and small inland water
202 bodies, and it generally occurs where salinity is <10 (Meisch, 2000). Accordingly, the specific
203 conductivity tolerance of *Heterocypris salina* ranges between 2.8 and 8.2 mS cm⁻¹ and 0.7
204 and 5.9 mS cm⁻¹, as determined from the occurrence of this species in 37 water bodies in
205 Israel and at 43 sites in Spain, respectively (Mezquita et al., 2005; Mischke et al., 2010).

206 *Eucyprinotus rostratus* was recorded from few freshwater sites in Europe, Turkey and the
207 Near East (Martens et al., 1992, 2002; Martens and Ortal, 1999; Eitam et al., 2004; Tunoğlu

208 and Ertekin, 2008; Mischke et al., 2010). We assume that the few shells of *Heterocypris*
209 *salina* and *Eucyprinotus* cf. *rostratus* originated from small fresh to slightly brackish water
210 bodies on **the** Hersek Peninsula. Three out of four samples containing charophyte
211 gyrogonites correspond to the upper two shell layers (Fig. 2). Although charophytes may
212 occur at relatively high salinities too, the coinciding occurrence of the non-marine ostracods
213 and the charophyte remains suggests that the gyrogonites were probably transported from
214 more marginal, less brackish positions in the lagoon or from small fresh to slightly brackish
215 water bodies on the peninsula.

216 The simultaneous occurrence of ostracods of different origin (lagoonal: *C. torosa* and
217 *Loxococoncha elliptica*; shallow marine: *L. rhomboidea*, *Xestoleberis* sp., *Pontocythere* sp. and
218 *Aurila* cf. *arborescens*; and inland waters: *H. salina* and *E. cf. rostratus*) within beds of
219 brackish-marine mollusc shells and fragments indicates that the shell layers were deposited
220 under high-energy environmental conditions (Ruiz et al., 2010). In the case of Lake Manyas
221 (140 km west of Hersek Lagoon), ostracods of different origins also are interpreted as
222 reflecting an event of large amplitude (seiche) leading to a spatially averaged snapshot of
223 regional assemblages (Leroy et al., 2002).

224 The shell layers are separated by homogenous mud of ca 40 cm thickness suggesting three
225 distinct events. Tsunamis or large storms are the two main processes which may have
226 turned the sheltered setting of Hersek lagoon into a high-energy depositional environment.

227 The occurrence of shells of two species from only slightly brackish or even freshwater
228 habitats implies that there was not only a landward transport of marine ostracod shells but
229 also a seaward transport of non-marine shells. Since tsunamis have generally a larger inland
230 extent than storms (Dawson and Stewart, 2007; Kortekaas and Dawson, 2007), we assume
231 that the shallow marine ostracod shells were transported to Hersek Lagoon during the run-up
232 phase and the non-marine ostracod shells during the backwash phase of tsunamis although
233 this differentiation between tsunamis and large storms as the triggering processes for the
234 high-energy deposits in Hersek Lagoon remains speculative.

235 Alternatively, the occurrence of ostracod shells from inland waters in Hersek lagoon could be
236 explained by transport and deposition from the **Yalak** River (Fig. 1). There are however four
237 arguments against this assumption: (1) the present disconnection between the **Yalak** River
238 and Hersek Lagoon existed apparently during the entire period covered by the investigated
239 core and additional cores from **the** Hersek Lagoon as revealed from clay mineral analysis by
240 Bertrand et al. (submitted), (2) there is no evidence for the delivery of terrestrial plant matter
241 occurring as charred or non-charred plant remains within the three shell beds, (3) the > 500
242 μm grain size fraction shows rapid changes associated with the shells beds rather than
243 gradual changes expected for the accumulation of more proximal or distal delta sediments in
244 a lagoon, and (4) the occurrence of especially *Heterocypris salina* in somewhat higher
245 abundances apparently coincides systematically with the occurrence of the shallow marine
246 ostracods in the core. Thus, delivery of the non-marine ostracod shells by the **Yalakdere** to
247 the core site is unlikely.

248 In addition, transport to the core site of non-marine ostracod shells originating from the
249 erosion of Quaternary sediments of Hersek Peninsula is regarded as an unlikely process due
250 to the intense weathering of the exposed Quaternary sediments and to the expected poor
251 preservation or destruction of the fragile calcitic ostracods shells. The recorded non-marine
252 ostracod shells do not display a difference in shell preservation in comparison to the shells
253 with lagoonal and shallow marine origins. Although the incorporation of non-marine ostracod
254 shells from eroded Quaternary sediments cannot completely be ruled out based on the
255 available data, we do not consider this scenario as a realistic option.

256 The inferred shift from a coastal wetland to a lagoon in ca AD 800 probably resulted from
257 coseismic subsidence of part of the Hersek Peninsula, which was most likely triggered by the
258 historically documented AD 740 earthquake with a magnitude of 7.1 in the Marmara Sea
259 region (Ambraseys, 2002). This inference and results from additional cores in Hersek lagoon
260 are presented in Bertrand et al. (submitted). Three further earthquakes with magnitudes ≥ 6.8
261 were documented in AD 823, 860 and 869 (Ambraseys, 2002). However, the lack of

262 historical records for earthquake-induced tsunamis and the insufficient precision of our age-
263 depth model does not allow an unequivocal assignment of the three shell beds to these
264 earthquakes.

265 To conclude, our study of Hersek Lagoon sediments exemplified the great potential of
266 ostracods as indicators of tsunamis or large storms through several lines of evidence: (1) the
267 large number of ostracod shells accumulated during the high-energy events, (2) the higher
268 number of taxa which is not typical for an undisturbed lagoon setting, and (3) the mixture of
269 ostracod shells with clear marine, lagoonal and non-marine origins, i.e. spatial average. This
270 last criterion might help to differentiate between tsunami and storm deposits in appropriate
271 coastal settings with near-shore water bodies.

272

273 **Acknowledgements**

274 Funding was provided by the European Union in the framework of the REL.I.E.F. (RELIable
275 Information on Earthquake Faulting) project (EVG1-CT-2002-00069). We are grateful to Lisa
276 Doner and Serdar Aykuz (both Istanbul Technical University), Pedro Costa (Brunel
277 University), Salim Öncel (Gebze Institute of Technology), Özden Ileri and Fatih Uysal
278 (Ankara University) for assistance during our fieldwork expeditions in Turkey, to Lina Mehta,
279 Vanessa Tomasz and Paul Szadorsky for laboratory assistance at Brunel University, and to
280 Nerdin Kubanç for comments with respect to *Loxoconcha elliptica* specimens. We would also
281 like to thank Peter Frenzel and an anonymous reviewer for critical and very helpful
282 comments on a previous version of this manuscript, and Norm Catto for editorial help.

283

284 **References**

285 Altinsaçlı, S., 2004. Investigation on Ostracoda (Crustacea) fauna of some important
286 wetlands of Turkey. Pakistan Journal of Biological Sciences 7, 2130-2134.

- 287 Alvarez-Zarikian, C.A., Soter, S., Katsonopoulou, D., 2008. Recurrent submergence and
288 uplift in the area of ancient Helike, Gulf of Corinth, Greece: Microfaunal and
289 archaeological evidence. *Journal of Coastal Research* 24, 110-125.
- 290 Ambraseys, N., 2002. The seismic activity of the Marmara Sea region over the last 2000
291 years. *Bulletin of the Seismological Society of America* 92, 1-18.
- 292 Athersuch, J., Horne, D.J., Whittaker, J.E., 1989. Marine and Brackish Water Ostracods. In:
293 Kermack, D.M., Barnes, R.S.K. (Eds.), *Synopsis of the British Fauna (New Series)*, 43,
294 343 pp.
- 295 Bertrand, S., Doner, L., Cagatay, N., Akcer, S., Sancar, U., Schudack, U., Mischke, S.,
296 Leroy, S. Sedimentary record of coseismic subsidence in Hersek coastal lagoon (İzmit
297 Bay, Turkey) and the late Holocene activity of the North Anatolian Fault. submitted to
298 *Geochemistry, Geophysics, Geosystems* **Now where?**
- 299 Boomer, I., Waddington, C., Stevenson, T., Hamilton, D., 2007. Holocene coastal change
300 and geoarchaeology at Howick, Northumberland, UK. *The Holocene* 17, 89-104.
- 301 Clague, J.J., Hutchinson, I., Mathewes, R.W., Patterson, R.T., 1999. Evidence for late
302 Holocene tsunamis at Catala Lake, British Columbia. *Journal of Coastal Research* 15, 45-
303 60.
- 304 Dahanayake, K., Kulasekera, N., 2008. Recognition of diagnostic criteria for recent- and paleo-
305 tsunami sediments from Sri Lanka. *Marine Geology* 254, 180-186.
- 306 Dawson, A.G., Stewart, I., 2007. Tsunami deposits in the geological record. *Sedimentary*
307 *Geology* 200, 166-183.
- 308 Dawson, S., 2007. Diatom biostratigraphy of tsunami deposits: Examples from the 1998
309 Papua New Guinea tsunami. *Sedimentary Geology* 200, 328-335.
- 310 Dawson, S., Smith, D.E., 2000. The sedimentology of Middle Holocene tsunami facies in
311 northern Sutherland, Scotland, UK. *Marine Geology* 170, 69-79.
- 312 Dolu, E., Gökaşan, E., Meriç, E., Ergin, M., Görüm, T., Tur, H., Ecevitöglu, B., Avşar, N.,
313 Görmüş, M., Batuk, F., Tok, B., Çetin, O., 2007. Quaternary evolution of the Gulf of İzmit

314 (NW Turkey): A sedimentary basin under control of the North Anatolian Fault Zone. *Geo-*
315 *Marine Letters* 27, 355-381.

316 Dominey-Howes, D., 2007. Geological and historical records of tsunami in Australia. *Marine*
317 *Geology* 239, 99-123.

318 Donato, S.V., Reinhardt, E.G, Boyce, J.I, Rothaus, R., Vosmer, T., 2008. Identifying tsunami
319 deposits using bivalve shell taphonomy. *Geology* 36, 199-202.

320 Eitam, A., Blaustein, L., Van Damme, K., Dumont, H.J., Martens, K., 2004. Crustacean
321 species richness in temporary pools: relationships with habitat traits. *Hydrobiologia* 525,
322 125-130.

323 Frenzel, P., Boomer, I., 2005. The use of ostracods from marginal marine, brackish waters
324 as bioindicators of modern and Quaternary environmental change. *Palaeogeography,*
325 *Palaeoclimatology, Palaeoecology* 225, 68-92.

326 Fujino, S., Naruse, H., Matsumoto, D., Jarupongsakul, T., Sphawajruksakul, A., Sakakura,
327 N., 2009. Stratigraphic evidence for pre-2004 tsunamis in southwestern Thailand. *Marine*
328 *Geology* 262, 25-28.

329 Fujiwara, O., Masuda, F., Sakai, T., Irizuki, T., Fuse, K., 2000. Tsunami deposits in Holocene
330 bay mud in southern Kanto region, Pacific coast of central Japan. *Sedimentary Geology*
331 135, 219-230.

332 Kortekaas, S., Dawson, A.G., 2007. Distinguishing tsunami and storm deposits: An example
333 from Martinhal, SW Portugal. *Sedimentary Geology* 200, 208-221.

334 Kozacı, Ö., 2002. Hersek deltasi'nda Kuzey Anadolu fayi'nin Yalova segmenti üzerinde
335 paleosismolojik calismalar. Unpublished bachelor thesis, Istanbul Technical University,
336 Turkey.

337 Kubanç, C., Meriç, E., Gülen, D., 1999. *Urocythereis britannica* Athersuch'nın İzmit Körfezi
338 (KB Türkiye) Pleyistosen'inde Bulunuşu Üzerine. *Turkish Journal of Zoology* 23, 791-799.

339 Kubanç, S.N., 2005. Diversity and comparison of Ostracoda of South Marmara Sea. *Journal*
340 *of the Black Sea/Mediterranean Environment* 11, 257-275.

341 Kuşçu, I., Okamura, M., Matsuoka, H., Awata, Y., 2002. Active faults in the Gulf of
342 İzmit on the North Anatolian Fault, NW Turkey: A high-resolution shallow seismic
343 study. *Marine Geology* 190, 421-443.

344 Leroy, S., Kazancı, N., Ileri, Ö., Kibar, M., Emre, O., McGee, E., Griffiths, H.I., 2002. Abrupt
345 environmental changes within a late Holocene lacustrine sequence south of the Marmara
346 Sea (Lake Manyas, N-W Turkey): possible links with seismic events. *Marine Geology* 190,
347 531-552.

348 Leroy, S.A.G., Warny, S., Lahijani, H., Piovano, E., Fanetti, D., Berger, A.R., 2010. The role
349 of geosciences in the improvement of mitigation of natural disasters: five case studies. In:
350 Beer, T. (Ed.), *Geophysical Hazards: Minimising risk, maximising awareness*. Springer
351 Science series International Year of Planet Earth, pp. 115-147.

352 Lettis, W., Bachluber, J., Witter, R., Brankman, C., Randolph, C.E., Barka, A., Page, W.D.,
353 Kaya, A., 2002. Influence of releasing step-overs on surface fault rupture and fault
354 segmentation: Examples from the 17August 1999 Izmit earthquake on the North Anatolian
355 Fault, Turkey. *Bulletin of the Seismological Society of America* 92, 19-42.

356 Maramai, A., Graziani, L., Tinti, S., 2005. Tsunamis in the Aeolian Islands (southern Italy): a
357 review. *Marine Geology* 215, 11-21.

358 Martens, K., Ortal, R., 1999. Diversity and zoogeography of inland-water Ostracoda
359 (Crustacea) in Israel (Levant). *Israel Journal of Zoology* 45, 159-173.

360 Martens, K., Ortal, R., Meisch, C., 1992. The ostracod fauna of Mamilla Pool (Jerusalem,
361 Israel) (Crustacea, Ostracoda). *Zoology in the Middle East* 7, 95-114.

362 Martens, K., Schwartz, S.S., Meisch, C., Blaustein, L., 2002. Non-marine Ostracoda
363 (Crustacea) of Mount Carmel (Israel), with taxonomic notes on Eucypridinae and circum-
364 mediterranean *Heterocypris*. *Israel Journal of Zoology* 48, 53-70.

365 Meisch, C., 2000. *Freshwater Ostracoda of Western and Central Europe*. Spektrum,
366 Heidelberg, 522 pp.

367 Mezquita, F., Roca, J.R., Reed, J.M., Wansard, G., 2005. Quantifying species–environment
368 relationships in non-marine Ostracoda for ecological and palaeoecological studies:
369 Examples using Iberian data. *Palaeogeography, Palaeoclimatology, Palaeoecology* 225,
370 93-117.

371 Mischke, S., Almogi-Labin, A., Ortal, R., Schwab, M.J., Boomer, I., 2010. Quantitative
372 reconstruction of lake conductivity in the Quaternary of the Near East (Israel) using
373 ostracods. *Journal of Paleolimnology* 43, 667-688.

374 Morton, R.A., Gelfenbaum, G., Jaffe, B.E., 2007. Physical criteria for distinguishing sandy
375 tsunami and storm deposits using modern examples. *Sedimentary Geology* 200, 184-207.

376 Özaksoy, V., Emre, Ö., Yıldırım, C., Doğan, A., Özalp, S., Tokay, F., 2010.
377 Sedimentary record of late Holocene seismicity and uplift of Hersek restraining
378 bend along the North Anatolian Fault in the Gulf of İzmit. *Tectonophysics* 487, 33-
379 45.

380 Reimer, P.J., Baillie, M.G.L., Bard, E., Bayliss, A., Beck, J.W., Bertrand, C.H.J., Blackwell,
381 P.G., Buck, C.E., Burr, G.S., Cutler, K.B., Damon, P.E., Edwards, R.L., Fairbanks, R.G.,
382 Friedrich, M., Guilderson, T.P., Hogg, A.G., Hughen, K.A., Kromer, B., McCormac, G.,
383 Manning, S., Bronk Ramsey, C., Reimer, R.W., Plicht, J.v.d., Weyhenmeyer, C.E., 2004.
384 IntCal04 terrestrial radiocarbon age calibration, 0–26 cal kyr BP. *Radiocarbon* 46, 1029-
385 1058.

386 Ruiz, F., Abad, M., Cáceres, L.M., Vidal, J.R., Carretero, M.I., Pozo, M., Gonzáles-Regalado,
387 M.L., 2010. Ostracods as tsunami tracers in Holocene sequences. *Quaternary Research*
388 73, 130-135.

389 Ruiz, F., Gonzáles-Regalado, M.L., Baceta, J.I., Menegazzo-Vitturi, L., Pistolato, M.,
390 Rampazzo, G., Molinaroli, E., 2000. Los ostrácodos actuales de la laguna de Venecia (NE
391 de Italia). *Geobios* 33, 447-454.

392 Ruiz, F., Rodríguez-Ramírez, A., Cáceres, L.M., Vidal, J.R., Carretero, M.I., Abad, M., Olías,
393 M., Pozo, M., 2005. Evidence of high-energy events in the geological record: Mid-

394 Holocene evolution of the southwestern Donana National Park (SW Spain).
395 Palaeogeography, Palaeoclimatology, Palaeoecology 229, 212-229.
396 Tinti, S., Armigliato, A., Manucci, A., Pagnoni, G., Zaniboni, F., Yalçiner, A.C., Altinok, Y.,
397 2006. The generating mechanisms of the August 17, 1999 Izmit bay (Turkey) tsunami:
398 Regional (tectonic) and local (mass instabilities) causes. Marine Geology 225, 311-330.
399 Tunoğlu, C., Ertekin, I.K., 2008. Subrecent Ostracoda associations and the environmental
400 conditions of karstic travertine bridges on the Zamantý River, southern Turkey. Türkiye
401 Jeoloji Bülteni (Geological Bulletin of Turkey) 51, 151-171.
402 Ünlüatu, Ü., Oğuz, T., Latif, M.A., Özsoy, E., 1990. On the physical oceanography of the
403 Turkish Straits. In: Pratt, L.J. (Ed.), The Physical Oceanography of Sea Straits. Kluwer,
404 Dordrecht, pp. 25-60.
405 Witter, R., Lettis, W., Bachhuber, J., Barka, A., Evren, E., Cakir, Z., Page, D., Hengesh, J.,
406 Seitz, G., 2000. Paleoseismic Trenching Study Across the Yalova Segment of the North
407 Anatolian Fault, Hersek Peninsula, Turkey. In: Barka, A., Kazaci, O., Akyüz, S., Altunel, E.
408 (Eds.), The 1999 Izmit and Düzce Earthquakes: Preliminary Results. Istanbul Technical
409 University, Turkey, pp. 329-339.

410

411

412 **Figure and plate captions**

413 Fig. 1

414 Location of the coring site in Hersek Lagoon (arrow) at the northeastern side of Hersek
415 Delta/Peninsula. The study area is part of the Marmara Sea (inset), which is crossed by the
416 northern strand of the North Anatolian Fault (red lines). Geological units are represented
417 according to Witter et al. (2000) and Kozaci (2002), bathymetrical information according to
418 Lettis et al. (2002), and fault locations according to Kuşçu et al. (2002) and Özaksoy et al.
419 (2010). Figure modified from Bertrand et al (submitted).

420

421 Fig. 2

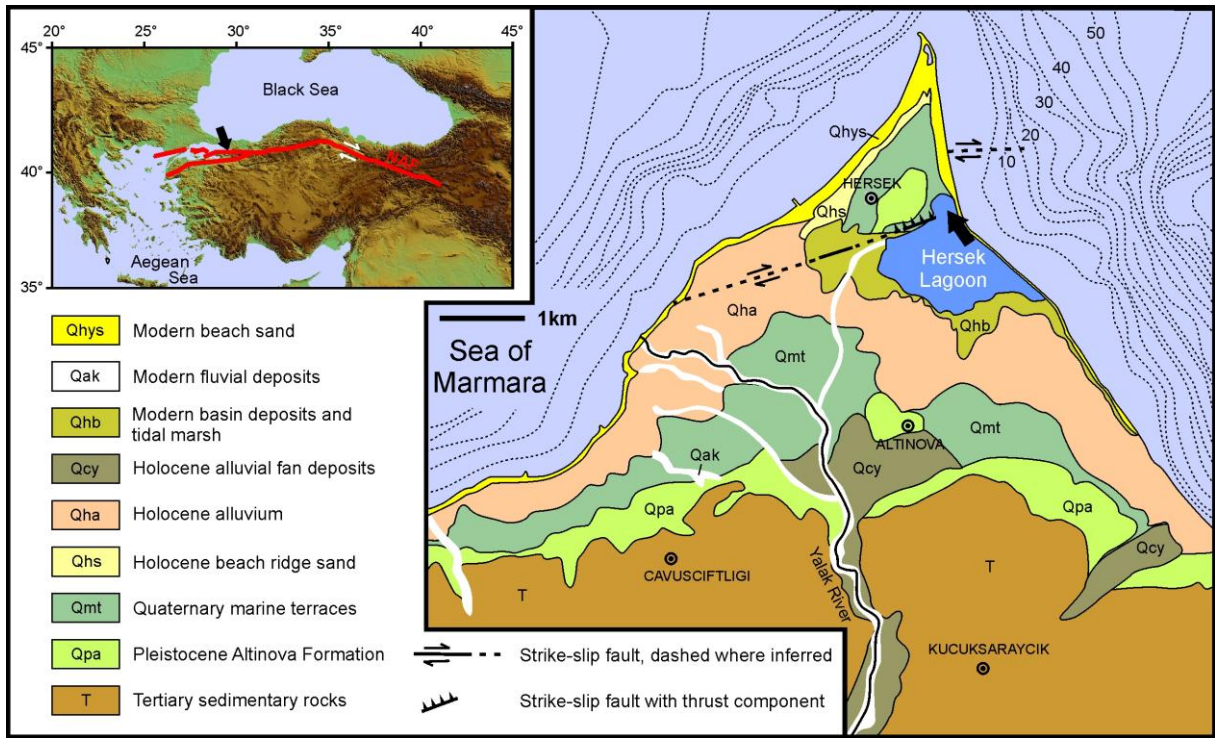
422 Ostracod abundance data, number of taxa and total number of shells per gram for the
423 investigated sediments from Hersek Lagoon (core HK04LV5). Hollow bars for *Cyprideis*
424 *torosa* represent ten times exaggerated results. Triangle next to the *Cyprideis torosa* column
425 indicates the position of the sole specimen of the noded form of the species *Cyprideis torosa*
426 forma *torosa* and the stars mark the samples for which the 250-500 µm sieve fractions were
427 not available. Core lithology, volumetric portions of particles >0.5 mm, and occurrence of
428 mollusc and plant remains are also indicated. Grey horizontal bars indicate high-energy
429 layers. ¹⁴C marks the location of samples used for radiocarbon dating.

430

431 Plate 1

432 Ostracod shells from Hersek Lagoon, core HK04LV5. 1-3 *Cyprideis torosa*, 1 female
433 carapace (Cp); 2 male Cp; 3 noded female Cp; 4 *Eucyprinotus* cf. *rostratus*, right valve (RV),
434 external view (ev); 5-6 *Loxoconcha* cf. *rhomboidea*, 5 juvenile (juv.) female left valve (LV),
435 internal view (iv); 6 juv. male RV, ev; 7 *Aurila* cf. *arborescens*, juv. RV, ev; 8-9 *Loxoconcha*
436 *elliptica*, 8 juv. female RV, ev, 9 juv. male LV, ev; 10 *Xestoleberis* sp., Cp; 11 *Heterocypris*
437 *salina*, LV, ev; 12 *Pontocythere* sp., juv. LV, iv. Specimens housed in the Institute of
438 Geological Sciences, Freie Universität Berlin, Germany.

439



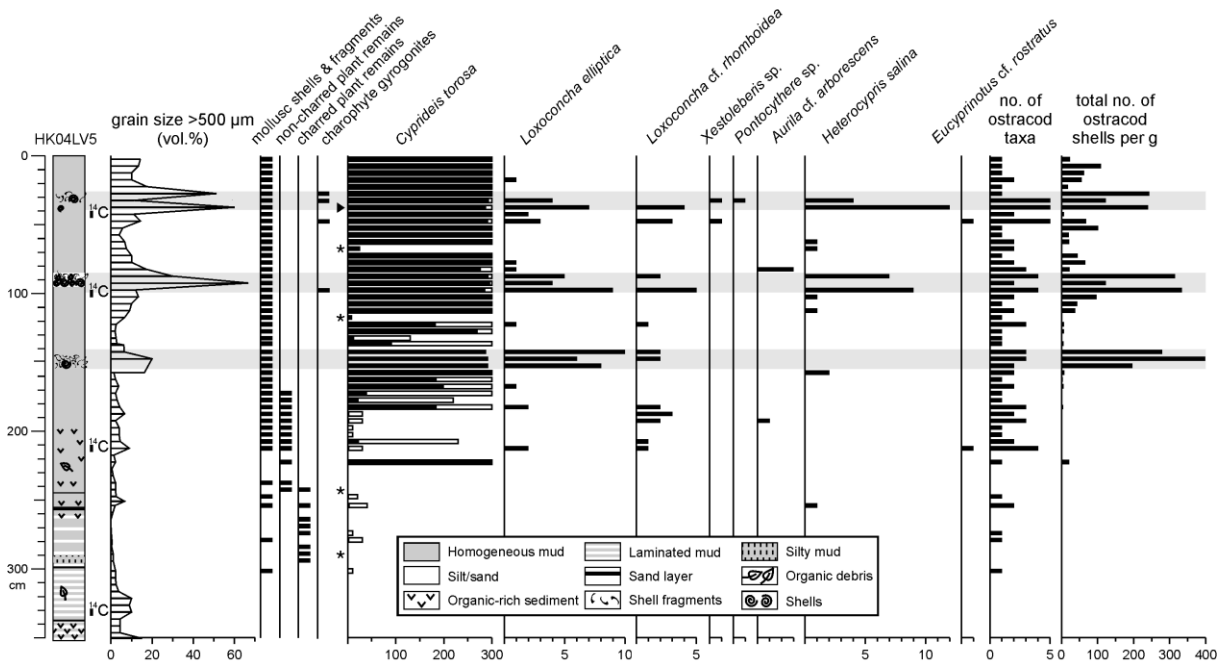
440

441

442

443

Figure 1

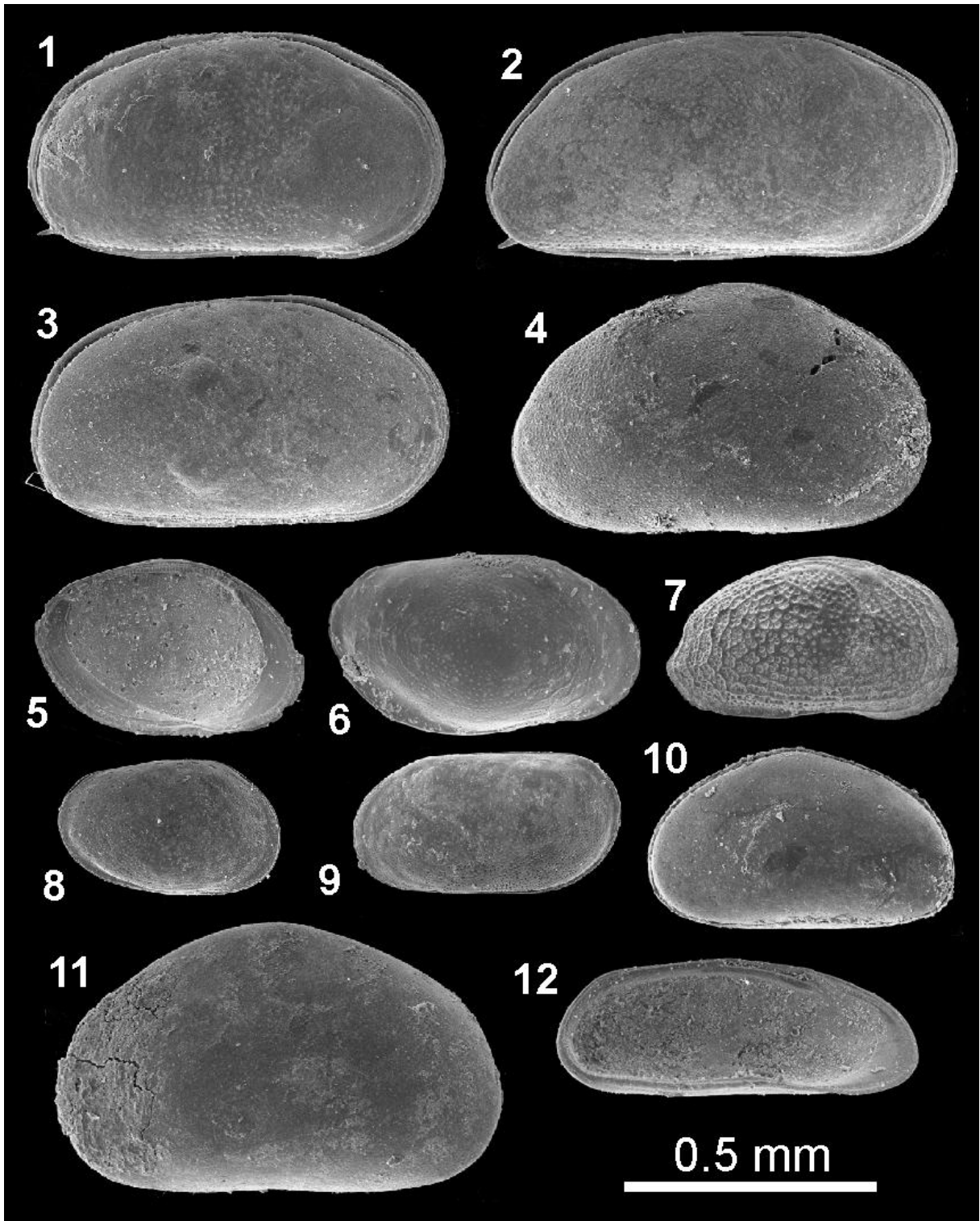


444

445

446

Figure 2



447

448

Plate 1. HK 05